SCIENTIFIC REPORTS
nature research

OPEN

Possible quantum critical behavior revealed by the critical current density of hole doped high-T_c cuprates in comparison to heavy fermion superconductors

S. H. Naqib* & R. S. Islam

The superconducting critical current density, J_c, in hole doped cuprates show strong dependence on the doped hole content, p, within the copper oxide plane(s). The doping dependent J_c mainly exhibits the variation of the intrinsic depairing critical current density as p is varied. $J_c(p)$ tends to peak at p ~ 0.185 in copper oxide superconductors. This particular value of the hole content, often termed as the critical hole concentration, has several features putative to a quantum critical point (QCP). Very recently, the pressure dependences of the superconducting transition temperature (T_c) and the critical current (I_c) in pure $CeRhIn_5$ and Sn doped $CeRhIn_5$ heavy fermion compounds have been reported (Nature Communications (2018) 9:44, https://doi.org/10.1038/s41467-018-02899-5). The critical pressure demarcates an antiferromagnetic quantum critical point where both T_c and I_c are maximized. We have compared and contrasted this behavior with those found for $Y_{1-x}Ca_xBa_2Cu_3O_{7-\delta}$ in this brief communication. The resemblance of the systematic behavior of the critical current with pressure and hole content between heavy fermion systems and hole doped cuprates is significant. This adds to the circumstantial evidence that quantum critical physics probably plays a notable role behind the unconventional normal and superconducting state properties of copper oxide superconductors.

It has been well over three decades since the discovery of superconductivity at high transition temperature in hole doped copper oxide materials in the mid-eighties[1,2]. The precise mechanism leading to Cooper pairing of the extra holes added to the CuO_2 planes of these strongly correlated electronic systems remains elusive till date[3–5]. A remarkable set of coexisting and often competing electronic ground states[3–7] in hole doped cuprates pose a serious theoretical challenge which the condensed matter physics community is yet to surmount. The standard theory for condensed matter physics, the Landau Fermi-liquid theory, breaks down completely in the case of underdoped (UD) cuprates[3–5]. The overdoped (OD) side is comparatively more conventional but still exhibits a number of anomalous characteristics[8].

In the absence of any agreed upon theoretical scheme to describe the Mott physics of undoped antiferromagnetic (AFM) insulating state and its eventual transformation to the pseudogapped normal state, charge and spin density ordered states, and d-wave superconductivity upon hole doping, in a coherent fashion, the cuprate research community has focused their attention in exploring various possible scaling relations and generic features found in these materials and in other strongly correlated electronic systems with non-Fermi liquid features[9–17]. These systematic studies of generic behaviors can provide us with important clues to unlock the mystery of the physics of electronic phase diagram of high-T_c cuprates in the normal and superconducting (SC) states.

Since late 1990s, it had been proposed that presence of a quantum critical point (QCP) in the T-p phase diagram could be responsible for unconventional charge and magnetic excitations that could possibly offer explanations for non Fermi-liquid like charge and magnetic transport properties of high T_c cuprates. The parameter p (often termed simply as *hole content* or *hole concentration*) signifies the number of doped holes per Cu atom in the CuO_2 plane. A QCP is understood via the concept of quantum phase transition (QPT). Unlike ordinary phase transitions driven by thermal energy, a QPT is characterized at a particular value of non-thermal parameter

Department of Physics, University of Rajshahi, Rajshahi, 6205, Bangladesh. *email: salehnaqib@yahoo.com

(e.g., critical hole content for cuprates) where a continuous phase transition takes place between a quantum disordered phase and a quantum ordered phase at zero temperature. The correlations at the QCP demonstrate spatio-temporal scale invariance. This implies that the poles present in the quasiparticle (QP) spectral function as predicted in the Fermi-liquid theory are absent here. Instead, one finds a power-law scaling behavior and the QP spectral function assumes a form given by (ω/T), where ω sets the energy scale of the quantum critical excitation mode. This leads to a dissipative QP relaxation time given by $h/(2\pi k_B T)$ which in turn implies that the scattering QP rate is linear in T. Moving away from the QCP, the energy scale for which scale invariance is valid, gradually increases[18]. It is worth mentioning that this T-linear QP scattering rate is considered as one of the prime signature of possible quantum criticality in hole doped cuprates[11–14] and other systems[18].

Quite interestingly the singular interactions arising from the competing phases at the QCP can provide with the 'glue' for Cooper pairing at high temperatures[19–21]. For example, Castellani *et al.*[19] presented a scenario where a QCP due to formation of incommensurate charge density waves roughly accounts for some of the generic features of the high-T_c cuprates, both in the normal and in the SC states, including a d-wave SC order parameter.

It should be mentioned that the presence and precise nature of a QCP in hole doped cuprates are hotly debated issues[22]. The situation is clearer in the case of heavy fermion (HF) and iron pnictide superconductors[22–24]. As far as SC HFs are concerned, $CeCu_2Si_2$ is the prime candidate for antiparamagnon mediated superconductivity near a spin density wave QCP[24]. Besides, superconductivity may emerge from the proximity to a magnetic field-induced QCP, like that in $CeCoIn_5$[25] and perhaps also in UBe_{13}[26]. The case for QCP in iron pnictides is quite strong. Evidence for superconductivity in at least one iron pnictide due to AFM quantum critical spin fluctuation is overwhelming[22,27]. Identification of the ground electronic state, its symmetry and thermodynamic signature of the symmetry breaking at the QCP in cuprates, on the other hand, are unclear[22] at the moment. Under the circumstances, a useful strategy is to compare and contrast various non-Fermi liquid like properties of cuprates with those of the HF and iron pnictide systems.

Very recently, Jung *et al.*[28] have studied the SC critical currents, I_c, in $CeRhIn_5$ and 4.4% Sn-doped $CeRhIn_5$ HF superconductors as a function of pressure (P). The I_{c0}s (zero-field critical currents) of these HF compounds under pressure exhibit a universal temperature dependence, underlining that the peak in zero-field $I_{c0}(P)$ is determined predominantly by quantum critical fluctuations associated with a hidden magnetic QCP at a critical pressure P_c, where superconducting transition temperature is also maximum. Motivated by this particular study[28], we have investigated the hole content dependent zero-field critical current density, J_{c0}, of a series of $Y_{1-x}Ca_xBa_2Cu_3O_{7-\delta}$ superconductors over wide range of compositions. We have also looked at the hole content dependent vortex activation energy and irreversibility field of $YBa_2CuO_{7-\delta}$ thin films in this investigation. The generic behaviors of the superconducting critical current density and vortex pinning characteristics in $Y_{1-x}Ca_xBa_2Cu_3O_{7-\delta}$ and Ce-based HF superconductors show strikingly similar behavior. We have discussed this feature and their possible implication in this short communication. This is the first comparative systematic study based on critical current density between hole doped cuprates and heavy fermion superconductors to the best of our knowledge.

The rest of the paper is organized as follows. A brief description of $Y_{1-x}Ca_xBa_2Cu_3O_{7-\delta}$ compounds and some details regarding the previous J_c and magnetic field dependent resistivity measurements are presented in Section 2. The results are presented and compared to those obtained for Ce-based HF superconductors in Section 3. Section 4 comprises of the discussion on the results and important conclusions of this study.

$Y_{1-x}Ca_xBa_2Cu_3O_{7-\delta}$ samples and measurements

High-quality c-axis oriented crystalline thin films of $Y_{1-x}Ca_xBa_2Cu_3O_{7-\delta}$ ($x = 0.00, 0.05, 0.10, 0.20$) were grown on $SrTiO_3$ substrates using the method of pulsed LASER ablation technique. Substrates of dimensions $5 \times 5 \times 1\,mm^3$ and $10 \times 5 \times 1\,mm^3$ were used. The thicknesses of the films lie within 2800 ± 300 Å. Details regarding the film preparation and characterization can be found in ref.[29]. Hole content within the CuO_2 planes were varied by two independent means. The oxygen deficiency, δ, in the $CuO_{1-\delta}$ chains were controlled via oxygen annealing at different temperatures and partial pressures. The Ca content, x, substituted for the Y atom in the charge reservoir layer also adds holes to the CuO_2 planes independent of the oxygen loading in the $CuO_{1-\delta}$ chains. This enables one to access the overdoped side relatively easily. Pure YBCO with fully oxygen loaded CuO chains can give a maximum p value ~ 0.180. Information about the annealing treatments and magnetization measurements of the thin films can be found in refs[29–31]. The hole content was estimated with high degree of accuracy from three different methods: room temperature thermopower (S[290 K])[32,33], c-axis lattice constant[30], and the well known parabolic $T_c(p)$ relation[34,35]. In this paper we have used the p-values obtained from the S[290 K] data. This is quite insensitive to the crystalline order and disorder content of the sample and depends solely on the number of doped holes in the CuO_2 plane. Details regarding the magnetic field dependent resistivity ($\rho_{ab}(H, T)$) measurements and analysis of the flux dynamics can be found in ref.[36]. All the measurements presented for $Y_{1-x}Ca_xBa_2Cu_3O_{7-\delta}$ in this study were done for the H II c configuration, where the supercurrent circulated in the CuO_2 plane. We have shown representative M-H loops for $Y_{1-x}Ca_xBa_2Cu_3O_{7-\delta}$ thin films at different temperatures and hole contents in Fig. 1. Representative $\rho_{ab}(H, T)$ data for $YBa_2Cu_3O_{7-\delta}$ thin films are shown in Fig. 2.

The zero-field critical current, J_{c0}, for the $Y_{1-x}Ca_xBa_2Cu_3O_{7-\delta}$ thin films with different amounts of Ca and oxygen deficiencies were calculated from the width of the magnetization loops at $H = 0$ G and the dimensions of the thin films following the method developed by Brandt and Indenbom[37] for finite geometry with the modified critical state model.

Hole Content Dependent Critical Current Density

The critical current density depends strongly on temperature. In this study, we have used the zero temperature critical current density for comparison. This was done by fitting the hole content dependent zero-field critical current density to the following relation[36,38]

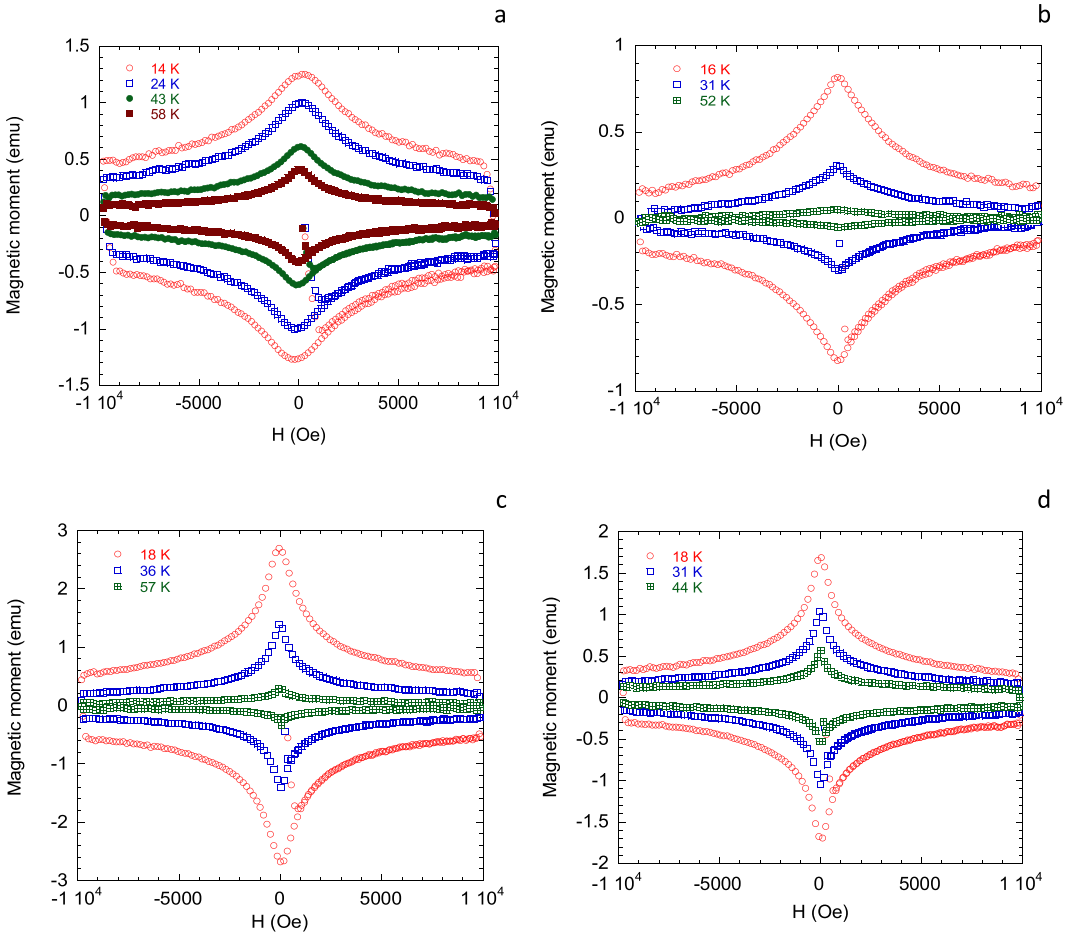

Figure 1. Representative magnetization loops for $Y_{1-x}Ca_xBa_2Cu_3O_{7-\delta}$ thin films with different compositions at different temperatures. The magnetic field was applied along *c*-direction. The sample compositions and hole contents are (**a**) $YBa_2Cu_3O_{7-\delta}$; $p = 0.162$, (**b**) $Y_{0.95}Ca_{0.05}Ba_2Cu_3O_{7-\delta}$; p = 0.123, (**c**) $Y_{0.90}Ca_{0.10}Ba_2Cu_3O_{7-\delta}$; p = 0.198, and (**d**) $Y_{0.80}Ca_{0.20}Ba_2Cu_3O_{7-\delta}$; p = 0.144. *p*-values are accurate within ±0.004. For clarity only one in twenty data points are shown.

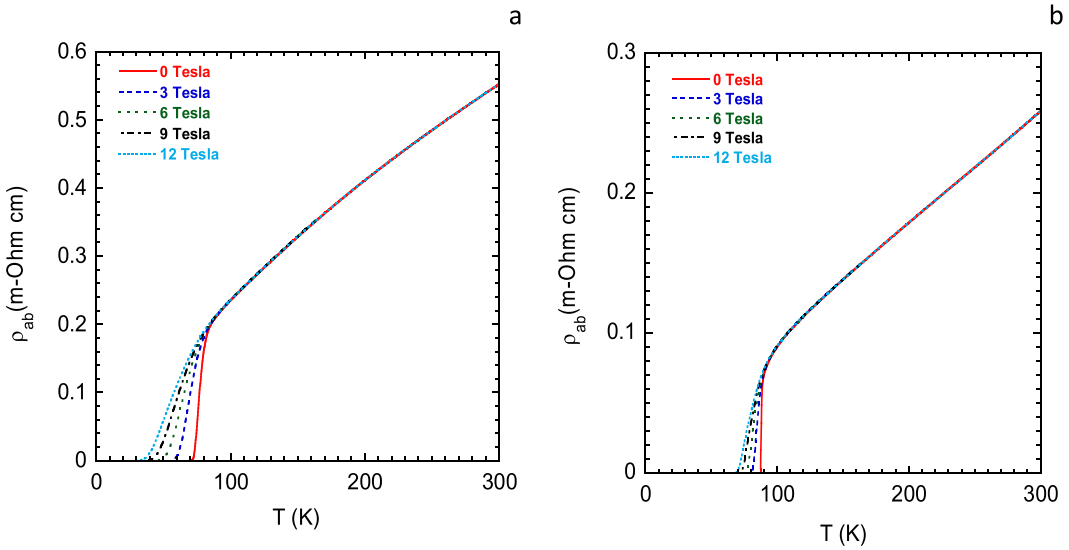

Figure 2. Representative magnetic field-dependent in-plane resistivity data for $YBa_2Cu_3O_{7-\delta}$ thin films with different hole contents. The magnetic fields were applied along the *c*-direction. The hole contents are (**a**) 0.118 and (**b**) 0.170. These values are accurate within ±0.004.

Compound	Hole content (p)	Critical current density, J_0 (10^6 A/cm^2)	Normalized critical current density
$YBa_2Cu_3O_{7-\delta}$	0.162	20.62	0.668*
	0.146	14.84	0.481*
	0.102	5.99	0.194*
$Y_{0.95}Ca_{0.05}Ba_2Cu_3O_{7-\delta}$	0.184	30.88	1.000
	0.170	26.04	0.843
	0.156	22.10	0.716
	0.123	12.10	0.392
$Y_{0.90}Ca_{0.10}Ba_2Cu_3O_{7-\delta}$	0.198	23.73	0.831
	0.188	28.54	1.000
	0.162	23.50	0.823
	0.160	24.41	0.855
	0.126	13.08	0.458
$Y_{0.80}Ca_{0.20}Ba_2Cu_3O_{7-\delta}$	0.201	17.08	0.921
	0.186	18.54	1.000
	0.166	17.01	0.917
	0.150	12.98	0.700
	0.144	12.03	0.649
	0.136	10.09	0.544

Table 1. Zero-field and zero-temperature critical current density of $Y_{1-x}Ca_xBa_2Cu_3O_{7-\delta}$ thin films. *Normalized with $J_0 = 30.88 \times 10^6$ A/cm^2. See Section 4 for details.

$$J_{c0}(t) = J_0(1 - t)^n \quad (1)$$

where, $t = (T/T_c)$, is the reduced temperature and J_0 is the extrapolated zero-field critical current density at $T = 0$ K. Value of the exponent, n, depends on the structural and electronic anisotropies, nature and distribution of defects, microstructure, level of homogeneity in composition, and details of flux pinning properties[38]. For the sample compositions used in this study, the values of n lie within the range 2.00 ± 0.60. The value of the exponent, n increases systematically with underdoping. The extracted values of J_0 for different hole contents are shown in Table 1.

We have plotted the normalized zero-temperature zero-field critical current density for $Y_{1-x}Ca_xBa_2Cu_3O_{7-\delta}$ thin films in Fig. 3. $J_0(p)$ has been normalized with the maximum value of J_0 for each Ca content (x). It is important to note that irrespective of the Ca content and oxygen deficiency in the $CuO_{1-\delta}$ chain, $J_0(p)$ is maximized when $p \sim 0.185$. We have also shown the normalized zero-field critical current for the 4.4% Sn-doped $CeRhIn_5$ HF superconductor as a function of pressure (P) in the inset. The systematic behavior of doped high-T_c cuprates and the HF compounds as functions of hole content and pressure are strikingly similar, as far as the critical current is concerned.

Next, we have shown the p-dependent behavior of the characteristic magnetic field, H_0, for $YBa_2Cu_3O_{7-\delta}$ thin films in Fig. 4. $H_0(p)$ gives a direct measure of the vortex activation energy and the irreversibility magnetic field[36,38–41]. Resistive broadening of the superconducting transition region as seen in Fig. 2, can be analyzed using the thermally assisted flux flow (TAFF) model[36,41]. The vortex activation energy, or equivalently the vortex pinning energy, $U(H, T)$, can be expressed quite well in a dimensionless form as follows: $U(T, H) = (1 - t)^m(H_0/H)^{-\beta}$. Here, $t = T/T_c$, the reduced temperature, β is a constant close to unity, and m is an exponent which varies with hole content, anisotropy and nature of the pinning centers within the sample. From the analysis of the $\rho_{ab}(H, T)$ data for $YBa_2Cu_3O_{7-\delta}$ thin films with different hole concentrations, $H_0(p)$ was calculated[36].

It is worth noting that both $J_0(p)$ and $H_0(p)$ changes with the doped hole content in the same fashion in $YBa_2Cu_3O_{7-\delta}$. Therefore, it is reasonable to assume that the p-dependent zero-field and zero-temperature critical current density in $Y_{1-x}Ca_xBa_2Cu_3O_{7-\delta}$ actually reflects the doping dependent vortex activation energy, which in turn is closely linked to the p-dependent SC condensation energy and superfluid density of the Cooper pairs[36,42].

Discussion and Conclusions

The normalized critical current density as a function of in-plane doped hole content of $Y_{1-x}Ca_xBa_2Cu_3O_{7-\delta}$ shows strong resemblance to the normalized critical current of $CeRhIn_5$ and 4.4% Sn-doped $CeRhIn_5$ HF superconductors as a function of pressure. For the high-T_c cuprate, critical current density peaks at $p_c \sim 0.185$, whereas for the 4.4% Sn-doped $CeRhIn_5$ HF compound the critical current peaks for $P_c \sim 1.35$ GPa. These particular values of the control parameters are known as the critical hole concentration and critical pressure, respectively. The importance of critical hole concentration in cuprates has been described in several earlier studies[13,21,22,43,44] in details. The widely investigated pseudogap in the quasiparticle energy spectrum tends to vanish abruptly at this particular hole content[13,21,43,44], the superfluid density and the superconducting condensation energy is maximized[21,43], the Fermi surface (FS) goes through a reconstruction[45], QP peaks appear abruptly in the normal state ARPES spectra[43], among others.

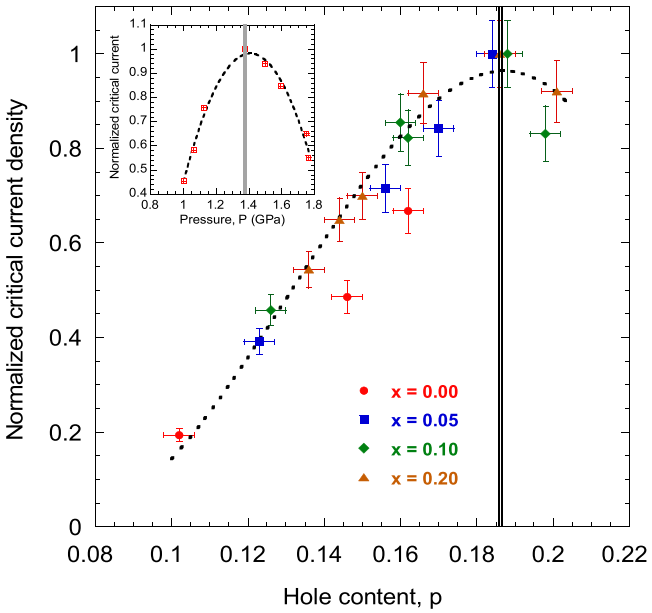

Figure 3. (Main) The normalized zero-temperature and zero-field critical current density of $Y_{1-x}Ca_xBa_2Cu_3O_{7-\delta}$ thin films as a function of doped hole content in the CuO_2 planes. The inset shows the variation of the normalized zero-field critical current of 4.4% Sn-doped $CeRhIn_5$ HF superconductor with pressure. The vertical lines mark the maximum critical currents and give the critical hole concentration and the critical pressure, at the putative quantum critical point. The dotted lines are fits to the data drawn as guides to the eyes.

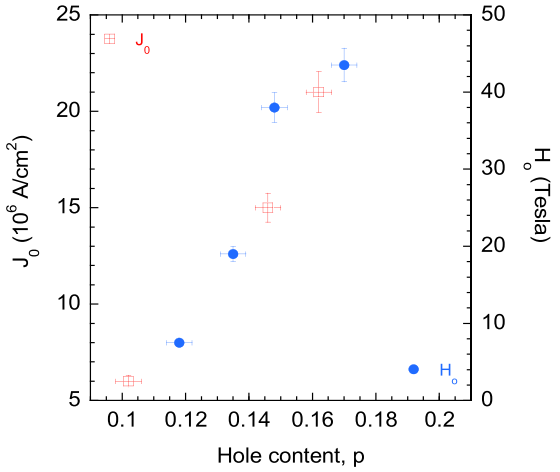

Figure 4. $J_0(p)$ and $H_0(p)$ of $YBa_2Cu_3O_{7-\delta}$ thin films.

Quantum criticality describes the collective excitations in strongly correlated systems undergoing a second-order phase transition at zero temperature. How these excitations can lead to formation of Cooper pairs is a matter of intense interest[46,47]. There are strong empirical evidences that spin density wave type quantum criticality can lead to superconductivity[22,24–26] but a coherent theoretical scheme is yet to be developed. In recent years a number of attempts have been made to formulate quantum critical SC theory to describe the high T_c and the non-FL behavior of copper oxide superconductors. Wang and Chubukov[20] have considered spin-mediated superconducting pairing at the antiferromagnetic QCP with an ordering momentum of $2k_F$ (k_F is the Fermi momentum). Kivelson *et al.*[48] studied the effect of soft critical collective fluctuations at a nematic quantum critical point on superconductivity. It was found that Cooper pairing channel is strengthened by such collective modes. Very recently Abanov *et al.*[49] considered a quantum-critical metal with interaction mediated by fluctuations of a critical order parameter. This interaction gives rise to two competing tendencies – Cooper pairing and non-Fermi liquid behavior, and seems to reproduce a number of anomalous features seen in the electronic phase diagram of hole doped cuprates. It is important to note that, irrespective of the details and the precise nature of the QCP[19,20,48,49], all these proposed models predict enhanced superconductivity at the QCP and therefore,

provides us with scenarios where the intrinsic critical current density is maximized at the QCP due to its dependence on the SC condensation energy and superfluid density.

For interested readers, some of the basic characteristics of the non-trivial QP excitations in strongly correlated electronic systems arising from the presence of QCPs have been described in greater detail in a related preprint of the current paper in ref.[50].

As far as the dome shaped $T_c(p)$ and $J_0(p)$ behaviors for hole doped cuprates are concerned, there are alternative scenarios that can roughly reproduce these features. For example, *t-J* model calculations can lead to dome shaped $T_c(p)$, and via the estimation of superfluid density, a dome shaped $J_0(p)$[51,52]. One particular drawback of such calculations is that it generally predicts a pseudogap line, the most prominent feature besides $T_c(p)$ in hole doped cuprates in the *T-p* phase diagram, that merges to the $T_c(p)$ line in the overdoped side[51]. Wealth of experimental results[7,12,13,16,21,35,43,44], on the other hand, indicate that the pseudogap vanishes quite abruptly below the superconducting dome at $p \sim 0.19$ for wide family of hole doped high-T_c cuprates[7,12,13,16,21,35,43,44]. This behavior finds strong and natural support within the QCP scenario[53]. In recent times, the pair density wave (PDW) scenario has attracted significant attention[54,55]. Within this particular scheme, the pairing order is periodic in space and fluctuating PDW order exists at high temperatures above T_c[54]. It is interesting to note that advanced theoretical calculations based on single band *t-J-U* model with charge density wave (CDW) and PDW have shown that a transition between the pure *d*-wave superconducting phase and the coexistent CDW+PDW phase can take place at $p \sim 0.18$ with modulated CDW and PDW orders located in the underdoped regime[55].

As in the hole doped high-T_c cuprates and some of the heavy-fermion compounds, superconductivity in iron pnictides emerges in close proximity to the AFM order[22,24,27,56], and T_c has dome-shaped dependence on doping or pressure. Electron-doped high-T_c cuprates are also consistent with the paradigm of an AFM QCP, with AFM order, FS reconstruction, and *T*-linear resistivity all manifested around a QCP at a particular critical doping ($x = x_c$) in $Nd_{2-x}Ce_xCuO_4$, $Pr_{2-x}Ce_xCuO_4$, and $La_{2-x}Ce_xCuO_4$[57]. In all these four systems close to the optimal T_c, various normal-state properties show a strong deviation from conventional Fermi liquid behavior. Such remarkable resemblance is highly unlikely to be coincidental. Furthermore, considerable theoretical efforts have been devoted into understanding of the (ω/T) scaling behavior of the dynamical susceptibility which is thought to be one of the prime features of the existence of an underlying QCP in the electronic phase diagram. Experimental optical conductivity data of optimally hole doped Bi2212 high-T_c cuprate exhibit such (ω/T) scaling over an extended region of temperature and energy[58]. This observation supports for quantum critical picture for hole doped cuprates. Therefore, although scenarios alternative to the one based on the QCP exist, the striking resemblance among the electronic phase diagrams of heavy fermions, iron pnictides, electron doped cuprates, and hole doped cuprates makes QCP a very viable framework for comprehensive understanding of the strange normal and superconducting state properties of high-T_c copper oxide superconductors.

It is worth noticing that in variety of SC systems[22,59] other than the hole doped cuprates, the quantum critical point coincides with the particular value of control parameter where the SC critical temperature is maximized. In most hole doped cuprates the optimum hole content, $p_{opt} \sim 0.16$, differs from the critical hole concentration, $p_c \sim 0.19$. This probably implies that one parameter scaling of quantum critical behavior is probably not adequate[60] in hole doped cuprates and a separate critical component competing with superconductivity may exist at $p_c \sim 0.19$.

It is not surprising to find that J_0 and the characteristic magnetic field H_0 follow the same *p*-dependence for $YBa_2Cu_3O_{7-\delta}$ thin films since H_0 gives a measure of the vortex activation energy[36,38–41]. We predict the similar pressure dependent behavior of the critical current density and vortex pinning energy for pure and doped $CeRhIn_5$ HF superconductors. This prediction results from the following arguments. It is reasonable to assume that the flux line is pinned at a site where the SC order parameter is partially or almost completely suppressed. In this situation the pinning energy of the vortex core would reveal itself as the energy barrier to motion of the flux line and therefore, would be equal to the flux activation energy U_0[39]. Here, U_0 denotes the zero temperature activation energy. It is this vortex activation energy that determines the critical current density and the irreversibility magnetic field[36,39]. By a heuristic scaling, Yeshurun and Malozemoff[61] and Tinkham[62] have shown that $U_0 \sim H_c^2$, where H_c is the thermodynamical critical magnetic field. The SC condensation energy, U_{sc} can also be expressed as $U_{sc} \sim H_c^2$. Therefore, $U_0 \sim U_{sc} \sim H_c^2$ [36,39]. Equivalently, the SC condensation energy can be expressed as $U_{sc} = N(E_F)\Delta_{sc}^2$, where $N(E_F)$ is the electronic energy density of states at the Fermi level and Δ_{sc} is the amplitude of the SC spectral gap. The quantity $N(E_F)\Delta_{sc}$ measures the Cooper pair number density. The SC coherence gap shows positive correlation with T_c. Therefore, it is logical to assume that in the presence of a QCP where T_c is maximized as in the case of HF superconductors, the critical current density, thermodynamical critical field and vortex activation energy should also be maximum. At other values of the non-thermal parameter, the variation of these critical current density related parameters should follow the variation in T_c. The arguments presented here are quite general in nature and do not depend significantly on the precise nature of the mechanism leading to Cooper pairing in a particular system.

It is perhaps instructive to notice that even though significant volume of work exists on critical current density of hole doped cuprates, systematic study of critical current density over a wide range of hole content extending from underdoped to overdoped regions of the phase diagram is highly scarce in literature. None of these few systematic studies[30,31,42,63,64] concerns itself explicitly with possible quantum critical physics in cuprates in relation to heavy fermion superconductors.

It should be noted that we have used the maximum value of J_0 of the 5% Ca substituted compound to normalize the critical current densities of the Ca-free thin film. This is done because these two films show almost similar physical properties including the residual resistivity, slope of the temperature dependent resistivity and SC transition temperature. For example, the maximum T_c at the optimum hole content ($p = 0.16$) for $Y_{1-x}Ca_xBa_2Cu_3O_{7-\delta}$ and $YBa_2Cu_3O_{7-\delta}$ thin films are 92.5 K and 91.0 K, respectively. This possibly introduces a small systematic error in the normalized critical current density of $YBa_2Cu_3O_{7-\delta}$. This error has no significant bearing on the conclusions drawn in this paper.

Data availability

The data sets generated and/or analyzed in this study are available from the corresponding author on reasonable request.

Received: 3 January 2019; Accepted: 2 October 2019;

Published online: 16 October 2019

References

1. Bednorz, J. G. & Müller, K. A. Possible high T_c superconductivity in the Ba−La−Cu−O system. Z. Phys. B: Condens. *Matter* **64**, 189 (1986).
2. Wu, M. K. *et al*. Superconductivity at 93 K in a new mixed-phase Y-Ba-Cu-O compound system at ambient pressure. *Phys. Rev. Lett.* **58**, 908 (1987).
3. Fradkin, E., Kivelson, S. A. & Tranquada, J. M. Theory of intertwined orders in high temperature superconductors. *Rev. Mod. Phys.* **87**, 457 (2015).
4. Lee, P. A., Nagaosa, N. & Wen, X.-G. Doping a Mott insulator: Physics of high- temperature superconductivity. *Rev. Mod. Phys.* **78**, 17 (2006).
5. Vishik, I. Photoemission perspective on pseudogap, superconducting fluctuations, and charge order in cuprates: a review of recent progress. *Rep. Prog. Phys.* **81**, 062501 (2018).
6. Kivelson, S. A. *et al*. How to detect fluctuating stripes in the high-temperature superconductors. *Rev. Mod. Phys.* **75**, 1201 (2003).
7. Tallon, J. L., Islam, R. S., Storey, J., Williams, G. V. M. & Cooper, J. R. Isotope Effect in the Superfluid Density of High-Temperature Superconducting Cuprates: Stripes, Pseudogap, and Impurities. *Phys. Rev. Lett.* **94**, 237002 (2005).
8. Le Tacon, M. *et al*. Dispersive spin excitations in highly overdoped cuprates revealed by resonant inelastic x-ray scattering. *Phys. Rev. B* **88**, 020501 (2013).
9. Uemura, Y. J. *et al*. Basic similarities among cuprate, bismuthate, organic, Chevrel- phase, and heavy-fermion superconductors shown by penetration-depth measurements. *Phys. Rev. Lett.* **66**, 2665 (1991).
10. Tallon, J. L., Cooper, J. R., Naqib, S. H. & Loram, J. W. Scaling relation for the superfluid density of cuprate superconductors: Origins and limits. *Phys. Rev. B* **73**, 180504 (2006).
11. Batlogg, B. *et al*. Normal state phase diagram of $(La,Sr)_2CuO_4$ from charge and spin dynamics. *Physica C* **235–240**, 130 (1994).
12. Naqib, S. H., Azam, M. A., Uddin, M. B. & Cole, J. R. A simple model for normal state in- and out-of-plane resistivities of hole doped cuprates. *Physica C* **524**, 18–23 (2016).
13. Naqib, S. H., Cooper, J. R., Tallon, J. L. & Panagopoulos, C. Temperature dependence of electrical resistivity of high-T_c cuprates – from pseudogap to overdoped regions. *Physica C* **387**, 365–372 (2003).
14. Naqib, S. H., Cooper, J. R., Islam, R. S. & Tallon, J. L. Anomalous Pseudogap and Superconducting State Properties in Heavily Disordered $Y_{1-x}Ca_xBa_2(Cu_{1-y}Zn_y)_3O_{7-\delta}$. *Phys. Rev. B* **71**, 184510 (2005).
15. LeBoeuf, D. *et al*. Electron pockets in the Fermi surface of hole-doped high-T_c superconductors. *Nature* **450**, 533 (2007).
16. Islam, R. S. & Naqib, S. H. Zn-induced in-gap electronic states in La214 probed by uniform magnetic susceptibility: relevance to the suppression of superconducting T_c. *Supercond. Sci. Technol.* **31**, 025004 (2018).
17. Kokanović, I., Cooper, J. R., Naqib, S. H., Islam, R. S. & Chakalov, R. A. Effect of Zn substitution on the normal-State magnetoresistivity of epitaxial $Y_{0.95}Ca_{0.05}Ba_2(Cu_{1-x}Zn_x)_3O_y$ and $Y_{0.9}Ca_{0.1}Ba_2Cu_3O_y$ films. *Phys. Rev. B* **73**, 184509 (2006).
18. Keimer, B., Kivelson, S. A., Norman, M. R., Uchida, S. & Zaanen, J. From quantum matter to high-temperature superconductivity in copper oxides. *Nature* **518**, 179 (2015).
19. Castellani, C., Di Castro, C. & Grilli, M. Non-Fermi-liquid behavior and d-wave superconductivity near the charge-density-wave quantum critical point. *Z. Phys. B* **103**, 137–144 (1997).
20. Wang, Y. & Chubukov, A. Quantum-critical pairing in electron-doped cuprates. *Phys. Rev. B* **88**, 024516 (2013).
21. Tallon, J. L. *et al*. Critical Doping in Overdoped High-T_c Superconductors: a Quantum Critical Point? *phys. stat. sol. (b)* **215**, 531 (1999).
22. Hussey, N. E., Buhot, J. & Licciardello, S. A Tale of Two Metals: contrasting criticalities in the pnictides and hole-doped cuprates. *Rep. Prog. Phys.* **81**, 052501 (2018).
23. Schroder, A. *et al*. Onset of antiferromagnetism in heavy-fermion metals. *Nature* **407**, 351–355 (2000).
24. Lévy, F., Sheikin, I., Grenier, B. & Huxley, A. D. Magnetic field-induced superconductivity in the ferromagnet URhGe. *Science* **309**, 1343–1346 (2005).
25. Petrovic, C. *et al*. Heavy-fermion superconductivity in $CeCoIn_5$ at 2.3 K. J. Phys.: Cond. *Matter* **13**, L337–L342 (2001).
26. Gegenwart, P. *et al*. Non-Fermi liquid normal state of the heavy-fermion superconductor UBe_{13}. *Physica C* **408–410**, 157–160 (2004).
27. James, G. A. *et al*. Transport near a quantum critical point in $BaFe_2(As_{1-x}P_x)_2$. *Nature Physics* **10**, 194–197 (2014).
28. Soon-Gil Jung *et al*. A peak in the critical current for quantum critical superconductors. *Nature communications*, https://doi.org/10.1038/s41467-018-02899-5 (2018).
29. Naqib, S. H., Chakalov, R. A. & Cooper, J. R. Structural and electrical properties of c-axis oriented $Y_{1-x}Ca_xBa_2(Cu_{1-y}Zn_y)_3O_{7-\delta}$ thin films grown by pulsed laser deposition. *Physica C* **407**, 73 (2004).
30. Naqib, S. H. & Semwal, A. Low-temperature critical current of $Y_{1-x}Ca_xBa_2Cu_3O_{7-\delta}$ thin films as a function of hole content and oxygen deficiency. *Physica C* **425**, 14 (2005).
31. Semwal, A. *et al*. Doping dependence of the critical current and irreversibility field in $Y_{1-x}Ca_xBa_2Cu_3O_{7-\delta}$. *Supercond. Sci. Technol.* **17**, S506 (2004).
32. Naqib, S. H. The Effect of Zn Substitution on the State of Oxygen Deficiency and Hole Concentration in $Y_{1-x}Ca_xBa_2(Cu_{1-y}Zn_y)_3O_{7-\delta}$. *Physica C* **443**, 43 (2006).
33. Tallon, J. L., Cooper, J. R., DeSilva, P. S. I. P. N., Williams, G. V. M. & Loram, J. L. Thermoelectric Power: A Simple, Instructive Probe of High-T_c Superconductors. *Phys. Rev. Lett.* **75**, 4114 (1995).
34. Presland, M. R., Tallon, J. L., Buckley, R. G., Liu, R. S. & Flower, N. E. General trends in oxygen stoichiometry effects on T_c in Bi and Tl superconductors. *Physica C* **176**, 95 (1991).
35. Naqib, S. H. Effect of Zn substitution on the suppression of T_c of $Y_{1-x}Ca_xBa_2(Cu_{1-y}Zn_y)_3O_{7-\delta}$ superconductors: pseudogap and the systematic shift of the optimum hole content. *Supercond. Sci. Tech.* **20**, 964 (2007).
36. Naqib, S. H. & Islam, R. S. Field-dependent resistive transitions in $YBa_2Cu_3O_{7-\delta}$: Influence of the pseudogap on vortex dynamics. *Chin. Phys. B* **24**, 017402 (2015).
37. Brandt, E. H. & Indenbom, M. Type-II-superconductor strip with current in a perpendicular magnetic field. *Phys. Rev. B* **48**, 12893 (1993).
38. Wai-Kwong Kwok *et al*. Vortices in high-performance high-temperature superconductors. *Rep. Prog. Phys.* **79**, 116501 (2016).
39. Zheng, D. N. *et al*. Magnetic susceptibilities, critical fields, and critical currents of Co- and Zn-doped $YBa_2Cu_3O_7$. *Phys. Rev. B* **49**, 1417 (1994).

40. Yeshurun, Y. & Malozemoff, A. P. Giant Flux Creep and Irreversibility in an Y-Ba-Cu-O Crystal: An Alternative to the Superconducting-Glass Model. *Phys. Rev. Lett.* **60**, 2202 (1988).
41. Xiaojun, X. *et al.* Dependence of activation energy upon magnetic field and temperature in $YBa_2Cu_3O_{7-\delta}$ epitaxial thin film. *Phys. Rev. B* **59**, 608 (1999).
42. Tallon, J. L. Thermodynamics and Critical Current Density in High-T_c Superconductors. *Ieee Transactions On Applied Superconductivity* **25**, 8000806 (2015).
43. Tallon, J. L. & Loram, J. W. The doping dependence of T^* - what is the real high- T_c phase diagram? *Physica C* **349**, 53 (2001).
44. Naqib, S. H., Cooper, J. R., Tallon, J. L., Islam, R. S. & Chakalov, R. A. The Doping Phase Diagram of $Y_{1-x}Ca_xBa_2(Cu_{1-y}Zn_y)_3O_{7-\delta}$ from Transport Measurements: Tracking the Pseudogap below T_c. *Phys. Rev. B* **71**, 054502 (2005).
45. Ramshaw, B. *et al.* A quantum critical point at the heart of high temperature superconductivity. *Science* **348**(6232), 317–320, https://doi.org/10.1126/science.aaa4990 (2015).
46. Sachdev, S. *Quantum Phase Transitions*. Cambridge University Press (2011).
47. Abanov, A., Chubukov, A. V. & Schmalian, J. Quantum-critical theory of the spin- fermion model and its application to cuprates: Normal state analysis. *Adv. Phys.* **52**, 119 (2003).
48. Lederer, S., Schattner, Y., Berg, E. & Kivelson, S. A. Enhancement of Superconductivity near a Nematic Quantum Critical Point. *Phys. Rev. Lett.* **114**, 097001 (2015).
49. Abanov, A., Yi-Ming, W., Wang, Y. & Chubukov, A. V. Superconductivity above a quantum critical point in a metal – gap closing vs gap filling, Fermi arcs, and pseudogap behavior. *arXiv* **1812**, 07634v1 (2018).
50. Naqib, S. H. & Islam, R. S. Critical current density of hole doped high-T_c cuprates and heavy fermion superconductors: relevance to the possible quantum critical behavior. *arXiv* **1812**, 10632 (2018).
51. Ogata, M. & Fukuyama, H. The *t–J* model for the oxide high-T_c superconductors. *Rep. Prog. Phys.* **71**, 036501 (2008).
52. Spalek, J., Zegrodnik, M. & Kaczmarczyk, J. Universal properties of high temperature superconductors from real space pairing: t-J-U model and its quantitative comparison with experiment. *Phys. Rev. B* **95**, 024506 (2017).
53. Varma, C. M. Pseudogap Phase and the Quantum-Critical Point in Copper-Oxide Metals. *Phys. Rev. Lett.* **83**, 3538–3541 (1998).
54. Dai, Z., Zhang, Y.-H., Senthil, T. & Lee, P. A. Pair-density waves, charge-density waves, and vortices in high-T_c cuprates. *Phys. Rev. B* **97**, 174511 (2017).
55. Zegrodnik, M. & Spalek, J. Incorporation of charge- and pair-density-wave states into the one-band model of d-wave superconductivity. *Phys. Rev. B* **98**, 155144 (2018).
56. Shibauchi, T., Carrington, A. & Matsuda, Y. A Quantum Critical Point Lying Beneath the Superconducting Dome in Iron Pnictides. *Annu. Rev. Condens. Matter Phys.* **5**, 113–35 (2014).
57. Proust, C. & Taillefer, L. The Remarkable Underlying Ground States of Cuprate Superconductors. Annu. Rev. Condens. *Matter Phys.* **10**, 409–29 (2019).
58. van der Marel, D. *et al.* Quantum critical behaviour in a high-T_c superconductor. *Nature* **425**, 271 (2003).
59. Gegenwart, P., Si, Q. & Steglich, F. Quantum Criticality in Heavy Fermion Metals. *Nature Physics* **4**, 186–197 (2008).
60. Phillips, P. & Chamon, C. Breakdown of One-Parameter Scaling in Quantum Critical Scenarios for High-Temperature Copper-Oxide Superconductors. *Phys. Rev. Lett.* **95**, 107002 (2005).
61. Yeshurun, Y. & Malozemoff, A. P. Giant Flux Creep and Irreversibility in an Y-Ba-Cu-0 Crystal: An Alternative to the Superconducting-Glass Model. *Phys. Rev. Lett.* **60**, 2202 (1988).
62. Tinkham, M. Resistive Transition of High-Temperature Superconductors. *Phys. Rev. Lett.* **61**, 1658 (1988).
63. Tallon, J. L., Williams, G. V. M. & Loram, J. W. Factors affecting the optimal design of high-T_c superconductors — the pseudogap and critical doping. *Physica C* **338**, 9–17 (2000).
64. Wen, H. H. *et al.* Hole doping dependence of the coherence length in $La_{2-x}Sr_xCuO_4$ thin films. *Europhys. Lett.* **64**, 790–796 (2003).

Acknowledgements

The authors would like to thank Dr. Anita Semwal for her part in the magnetization measurements.

Author contributions

S.H.N. designed the project and wrote the manuscript. S.H.N. and R.S.I. did the measurements and analyzed the data. Both the authors reviewed the manuscript.

Competing interests

The authors declare no competing interests.

Additional information

Correspondence and requests for materials should be addressed to S.H.N.

Reprints and permissions information is available at www.nature.com/reprints.

Publisher's note Springer Nature remains neutral with regard to jurisdictional claims in published maps and institutional affiliations.

Open Access This article is licensed under a Creative Commons Attribution 4.0 International License, which permits use, sharing, adaptation, distribution and reproduction in any medium or format, as long as you give appropriate credit to the original author(s) and the source, provide a link to the Creative Commons license, and indicate if changes were made. The images or other third party material in this article are included in the article's Creative Commons license, unless indicated otherwise in a credit line to the material. If material is not included in the article's Creative Commons license and your intended use is not permitted by statutory regulation or exceeds the permitted use, you will need to obtain permission directly from the copyright holder. To view a copy of this license, visit http://creativecommons.org/licenses/by/4.0/.

© The Author(s) 2019